INTERNATIONAL JOURNAL FOR NUMERICAL AND ANALYTICAL METHODS IN GEOMECHANICS
Int. J. Numer. Anal. Meth. Geomech., **23**, 217–241 (1999)

CONSTITUTIVE MODELLING OF A REINFORCED SOIL USING HIERARCHICAL MODEL

A. VARADARAJAN*†, K. G. SHARMA† AND K. M. SONI‡

Department of Civil Engineering, IIT Delhi, New Delhi-110 016, India

SUMMARY

Drained triaxial tests are conducted on natural and reinforced sand under various stress paths. Direct shear tests and pull-out tests are conducted on soil–reinforcement interface and on reinforcement, respectively. The effects of two types of reinforcement, viz, woven and non-woven geotextile and number of layers of reinforcement are investigated. Hierarchical single surface model is used to depict the behaviour of natural and reinforced soil by treating the soil as a single composite material and by considering soil, reinforcement and interface as independent elements. It is shown that the material parameters are very much affected by the type and the number of layers of reinforcement. The hierarchical model provides satisfactory prediction for both natural and reinforced soil. Copyright © 1999 John Wiley & Sons, Ltd.

Key words: reinforced soil; triaxial tests; elastoplastic theory; finite element method

1. INTRODUCTION

Reinforced soil is increasingly used in various structures such as earth retaining structures, embankments and foundations. The behaviour of reinforced soil is affected by a number of such factors as the characteristics of reinforcement, density, particle size and shape of soil, confining pressure and stress path. Modelling of the behaviour of reinforced soil is of considerable importance in the analysis and design of various structures. This paper deals with laboratory testing and constitutive modelling of a reinforced soil using a generalized elastoplastic model.

2. REVIEW

A number of studies have been conducted to understand the mechanism of reinforcement in soil and to provide models to predict the strength behaviour of reinforced soils (for example, References 1–3). A comprehensive review of these investigations is given by Soni.[4] Studies on modelling of the complete behaviour of the reinforced soil are very limited and are briefly reviewed herein. Sawicki[5] studied the behaviour of unidirectionally fibre reinforced soil assuming perfectly plastic Mohr–Coulomb failure criterion and associated flow rule. Madhav and

*Correspondence to: Professor A. Varadarajan, Department of Civil Engineering, Indian Institute of Technology, Hauz Khas, New Delhi 110016, India

† Professor
‡ Former Graduate Student

CCC 0363–9061/99/030217–25$17.50

Received 5 July 1997
Revised 26 March 1998

Poorooshasb[6] developed a foundation model element together with Winkler's springs. In this model, a rough membrane is proposed to simulate the reinforcement behaviour. Buhan and Siad,[7] considering the reinforced soil as a two-dimensional multilayer material made up of cohesionless soil, reinforcement layer and soil–reinforcement interface studied analytically the influence of a soil strip interface failure condition on the field strength of reinforced soil. Bourdeau[8] proposed a numerical model which was based on a two-dimensional plane strain model of the static equilibrium of an elastic membrane placed at the interface between a granular base and a compressible subgrade.

3. SCOPE

The scope of the investigation is to (i) conduct systematic laboratory tests on natural and reinforced soils using various types of reinforcement and reinforcement layers, (ii) use a generalized elastoplastic model based on hierarchical approach to characterise the behaviour of natural and reinforced soil considering (a) the reinforced soil as a single material and (b) the soil, the reinforcement and the interface as separate elements.

4. LABORATORY TESTS

Laboratory tests conists of (a) drained triaxial tests on 38 mm dia and 76 mm high cylindrical natural and reinforced soil samples, (b) direct shear tests on soil–reinforcement interface and (c) tension tests on reinforcement.

4.1. Materials

Ennore sand procured from the coastal area near Chennai in the southern part of Indian subcontinent has been used. This is also recognized as Indian standard sand for various purposes. The physical properties are similar to those of Ottawa sand and are: specific gravity = 2·64, uniformity coefficient = 1·63, effective size $D_{10} = 0{\cdot}40$ mm, median size $D_{50} = 0{\cdot}60$ mm, maximum and minimum dry densities are 18 and 16 kN/m^3, respectively. The soil particles are derived from quartz and are subrounded to rounded in shape.

For reinforcement, Geolon, a woven geotextile manufactured by Bombay Dyeing Company, India and needle punched non-woven geotextile manufactured by Shri Dinesh Mills Company, India, have been used. The characteristics of reinforcements, as determined by standard procedures, are given in Table I. Woven geotextile shows higher elastic modulus and higher yield strength than non-woven geotextile.

4.2. Tests

Triaxial tests have been conducted on (i) natural sand, (ii) reinforced sand with single layer of non-woven geotextile, placed at mid-height of sample (R1NW), (iii) reinforced sand with two layers of non-woven geotextile, placed at one-third and two-third heights of sample (R2NW) and (iv) reinforced sand with two layers of woven geotextile placed as above, R2W.

Triaxial tests have been conducted under seven stress paths as shown in Figure 1 on each of the four types of sand sample. Two or three confining pressures in the range of 100–300 kPa have been used for each stress path. A total of 62 tests have been conducted. Samples have been

Table I. Reinforcement properties

Properties	Non-woven geotextile	Woven geotextile
Material/colour	Polypropylene/white	Polypropylene/white
Thickness (mm)	2·8	0·64
Stiffness modulus (kN/m)	23·13	660
Yield strength (kN/m)	11·65	19·93

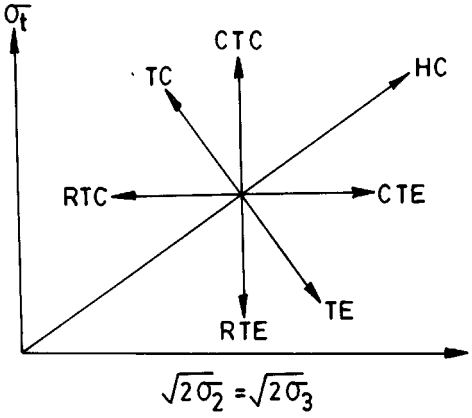

Figure 1. Stress paths used for the tests

prepared under saturated condition using split mould. A uniform system of tamping has been adopted to obtain same density for all the samples. Non-woven and woven geotextiles have been cut in the form of circular discs and placed in the soil samples at the required location during sample preparation.

Most of the triaxial tests have been conducted with a computer controlled triaxial testing equipment GDS Triaxial Testing System 38. This equipment has many features such as stress and strain controlled loading, stress path control, drainage control, compression and extension testing facility, data acquisition and interpretation. A few tests have been conducted with standard triaxial testing equipment.[9]

For the determination of interface friction between the soil and reinforcement, modified direct shear tests have been conducted on 6 cm × 6 cm size box.[10] The lower-half of the box contains a steel block over which geotextile is wrapped and fixed. The upper-half of the box is filled with dry soil. The tests have been conducted with normal stresses of 50, 100 and 150 kPa using a rate of displacement of 0·25 mm/min. From these tests shear stress–deformation responses have been determined.

The behaviour of geotextiles has been found by testing 10 samples each of woven and non-woven geotextile. Five tests in machine direction and five tests in cross-machine direction have been conducted using Hounsfield Universal Testing Machine (Model No. 50 KM). Elastic modulus and yield strength have been obtained from the tests.

5. CONSTITUTIVE MODEL

5.1. Natural and reinforced soil

Hierarchical single surface (HISS) model developed by Desai and his co-workers[11–16,18] has been chosen to characterize the behaviour of natural and reinforced soil. The attractive feature of this model is that a unified or hierarchical approach is adopted in the development to systematically include responses of progressive complexities such as isotropic hardening with associative flow rule and isotropic hardening with non-associative flow rule. This approach also enables simplification in the determination of material constants from laboratory tests and the number of constants as well.

The behaviour of reinforced soil is modelled in two ways: (a) as a single homogeneous material and (b) as a composite material consisting of sand, reinforcement and sand–reinforcement interface. For the interface, the specialized version of HISS model for joints and interfaces has been adopted. The details of these models are described briefly herein.

The continuous yielding and ultimate yield behaviour is given by a compact and specialized form of the general polynomial representation[11,12] as

$$F = \frac{J_{2D}}{p_a^2} - \left[-\alpha\left(\frac{J_1}{p_a}\right)^n + \gamma\left(\frac{J_1}{p_a}\right)^2 \right](1 - \beta S_r)^m = 0 \tag{1}$$

or

$$F = \bar{J}_{2D} - F_b F_s = 0 \tag{2}$$

where J_{2D} is the second invariant of the deviatoric stress tensor, J_1 is the first invariant of stress tensor, $\bar{J}_{2D} = J_{2D}/p_a^2$, p_a is the atmospheric pressure, γ, β and m are material response functions associated with the ultimate behaviour, α is the hardening function, n is the phase change parameter and S_r is the stress ratio given by

$$S_r = \frac{\sqrt{27}}{2}\frac{J_{3D}}{J_{2D}^{1.5}} \tag{3}$$

in which J_{3D} is the third invariant of deviatoric stress tensor. In equation (2), F_b is the basic function describing the shape of the yield function in $J_1 - \sqrt{J_{2D}}$ and F_s is the shape function which describes the shape in the octahedral plane.

The hardening function, α, is given by

$$\alpha = \frac{a_1}{\xi^{\eta_1}} \tag{4}$$

where, a_1 and η_1 are hardening parameters, and $\xi = \int (d\varepsilon_{ij}^P d\varepsilon_{ij}^P)^{1/2}$ is the trajectory of the plastic strains.

For the non-associative plasticity which is adopted herein, the plastic potential function, Q, is defined[12,13] as

$$Q = \frac{J_{2D}}{p_a^2} - \left[-\alpha_Q\left(\frac{J_1}{p_a}\right)^n + \gamma\left(\frac{J_1}{p_a}\right)^2 \right]F_s \tag{5}$$

where

$$\alpha_Q = \alpha + \kappa(\alpha_0 - \alpha)(1 - r_v) \tag{6}$$

in which $r_v = \xi_v/\xi$ and ξ_v is the volumetric part of ξ, α_0 is the value of α at the end of initial hydrostatic loading and κ is a non-associative parameter.

5.2. Soil–reinforcement interface

For the interface, the hierarchical model is specialized as[14,15]

$$F = \left(\frac{\tau}{p_a}\right)^2 + \alpha\left(\frac{\sigma_n}{p_a}\right)^n - \gamma\left(\frac{\sigma_n}{p_a}\right)^2 = 0 \tag{7}$$

where σ_n and τ are normal and shear stresses, respectively, and α, n and γ have similar meanings as in equation (1). In this case,

$$\xi = \int [\mathrm{d}v_r^2 + \mathrm{d}u_r^2]^{1/2} \tag{8}$$

where $\mathrm{d}v_r$ and $\mathrm{d}u_r$ are relative vertical and horizontal relative displacements.

The plastic potential is given by

$$Q = \left(\frac{\tau}{p_a}\right)^2 + \alpha_Q\left(\frac{\sigma_n}{p_a}\right)^n - \gamma\left(\frac{\sigma_n}{p_a}\right)^2 \tag{9}$$

where $\alpha_Q = \alpha + \kappa(\alpha_0 - \alpha)(1 - r_v)$ in which α_0 refers to the α value at the end of the application of normal stress.

5.3. Reinforcement

The elastoplastic behaviour of woven and non-woven reinforcements are modelled using von Mises yield criterion for the plasticity as

$$F = \sqrt{3J_{2D}} - \sigma_0 = 0 \tag{10}$$

where σ_0 is the yield strength.

6. MATERIAL PARAMETERS

6.1. Natural soil and reinforced soil

The procedure for the determination of material parameters has been described in detail in various references (for example, References 13, 16 and 18). It is briefly presented in the following:

At the ultimate condition, the hardening parameter, α, is zero and F can be arranged as

$$\left[\frac{J_{2D}}{J_1^2}\right]^{1/m} \gamma^{1/m} + \beta S_r = 1 \tag{11}$$

The value of m is found to be $-0{\cdot}5$ for many geologic materials. The values of γ and β are determined using ultimate stresses from stress–strain curves under various stress path tests.

The value of phase change parameter, n, is determined at the state of stress at which the plastic volume change is zero. At this condition,

$$n = \frac{2}{1 - (J_{2D}/J_1^2)(1/F_s\gamma)} \tag{12}$$

The value of n is obtained by averaging the values obtained from various tests.

The hardening parameters a_1 and η_1 are determined using Equation (4) from known α and ξ values at various stress levels of a test. The value of α is calculated by rearranging equation (1).

The averaged values of a_1 and η_1 in Equation (4) are obtained from various tests. The non-associative parameter, κ (equation (8)) is determined as follows:

$$\frac{d\varepsilon_v^P}{d\varepsilon_{11}^P} = \left(3\frac{\partial Q}{\partial J_1}\right) \Big/ \left(\frac{\partial Q}{\partial \sigma_{11}}\right) \tag{13}$$

where, $d\varepsilon_{11}^P$ is axial plastic strain increment, σ_{11} is axial stress and $d\varepsilon_v^P$ is volumetric plastic strain increment. The ratio of $d\varepsilon_v^P/d\varepsilon_{11}^P$ can be obtained from the slope of the observed $d\varepsilon_{11}^P$ vs. $d\varepsilon_v^P$ response by choosing a point in the ultimate state. The value of α_Q which is represented on the right-hand side of the equation (13) can then be found. Using this value along with α and r_v at ultimate condition, average values of κ are determined.

The Young's modulus, E, and Poisson's ratio, ν, are usually obtained from unloading slopes of stress–strain–volume change responses; however, here they are obtained approximately from the initial parts of the curves. The dependency of E on confining pressure is expressed using Janbu's[19] relationship as

$$E = kp_a\left(\frac{\sigma_3}{p_a}\right)^{n'} \tag{14}$$

where k and n' are the constants obtained from experimental results.

The material parameters have been determined by using the tests as follows: for natural and reinforced soils R1NW and R2NW, CTC test at $\sigma_c = 100$ and 200 kPa and TE test at $\sigma_c = 200$ kPa, for reinforced soil R2W, CTC test at $\sigma_c = 100$ kPa and RTE test at $\sigma_c = 200$ kPa. The material parameters for various soils are presented in Table II.

6.2. Soil–reinforcement interface

The details of determining material parameters are given by Fishman[20] and Desai and Fishman.[15] They are briefly presented herein.

At the ultimate condition, the growth function α being zero, the ultimate parameter γ is determined as

$$\gamma = \frac{\tau^2}{\sigma_n^2} \tag{15}$$

Noting that $\partial F/\partial\sigma_n = 0$ at phase change point, the parameter n is found from

$$\frac{\tau^2}{\sigma_n^2} = \gamma\left(1 - \frac{2}{n}\right) \tag{16}$$

Table II. Material parameters for natural and reinforced soils

Parameter	Natural soil	Reinforced soil R1NW	Reinforced soil R2NW	Reinforced soil R2W
Elastic constants				
k	600	500	230	690
n'	0·95	0·96	1·06	0·90
v	0·34	0·37	0·36	0·34
Ultimate parameters				
m	− 0·50	− 0·50	− 0·50	− 0·50
γ	0·071	0·072	0·088	0·089
β	0·610	0·687	0·727	0·667
Phase change parameter, n	2·54	2·98	3·07	2·90
Hardening parameters				
a_1	$0{\cdot}366 \times 10^{-3}$	$0{\cdot}405 \times 10^{-5}$	$0{\cdot}397 \times 10^{-4}$	$0{\cdot}273 \times 10^{-3}$
η_1	0·711	1·611	1·327	0·721
Non-associative parameter, κ	0·228	0·276	0·242	0·257

Table III. Material parameters of interface behaviour of non-woven and woven geotextile

Parameter		Non-woven geotextile	Woven geotextile
Elastic constants (kN/m^2/m)	K_s	3000	8000
	K_n	60000	90000
Ultimate parameters	γ	0·722	0·656
Phase change parameter	n	2·84	2·50
Hardening parameters	a_1	0·098	0·253
	η_1	0·675	0·241
Non-associative parameter	κ	0·875	0·802

The parameters a_1 and n_1 related to growth function (equation (4)) are found using the similar procedure used for soil by determining α and ξ at various stress levels.

The non-associative parameter, κ, is obtained as

$$\kappa = \frac{\alpha_Q}{\alpha_0(1 - r_v)} \tag{17}$$

where at ultimate condition

$$\alpha_Q = \left\{ \left[\frac{dv_r^P}{du_r^P} \right] 2\tau + 2\gamma \left(\frac{\sigma_n}{p_a} \right) \right\} \Big/ n \left(\frac{\sigma_n}{p_a} \right)^{n-1} \tag{18}$$

The elastic shear stiffness, K_s, is determined from the initial slope of the observed curve between τ and u_r. The elastic normal stiffness K_n is found as the initial slope of the observed relationship

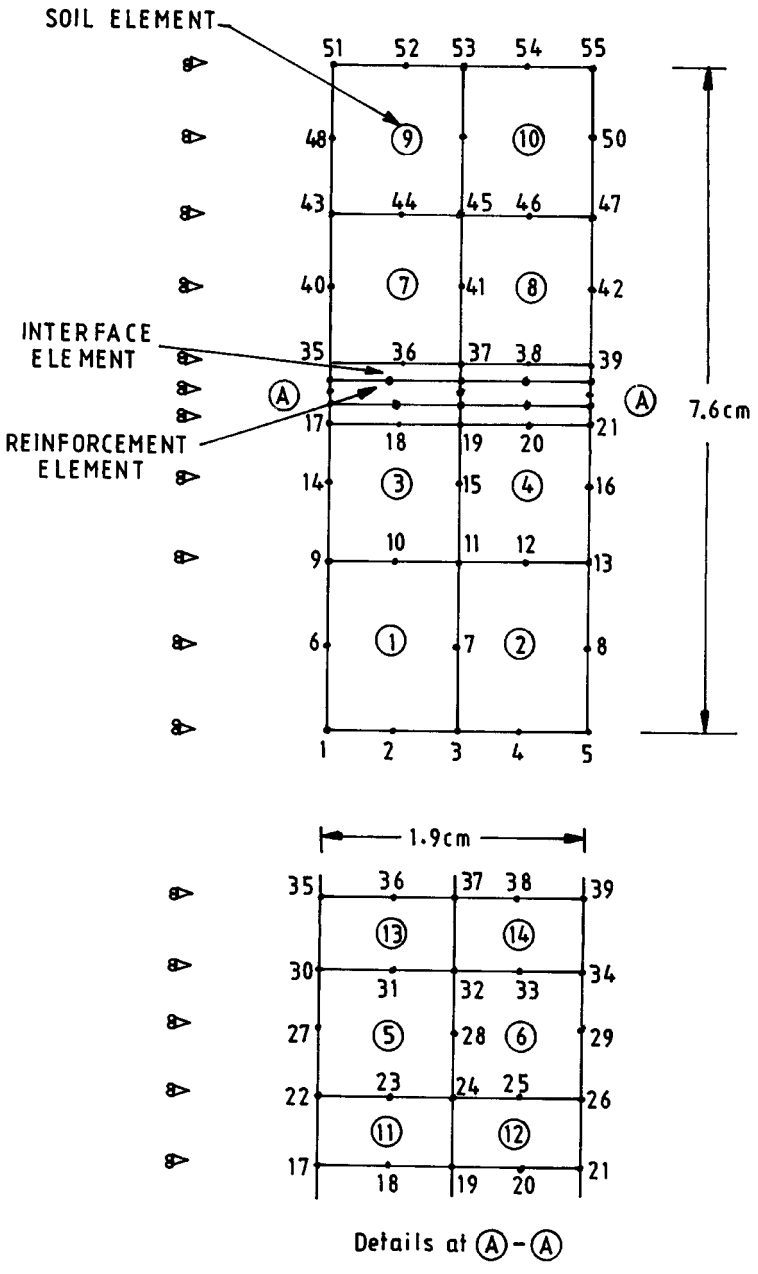

Figure 2. Finite element discretization of reinforced soil sample

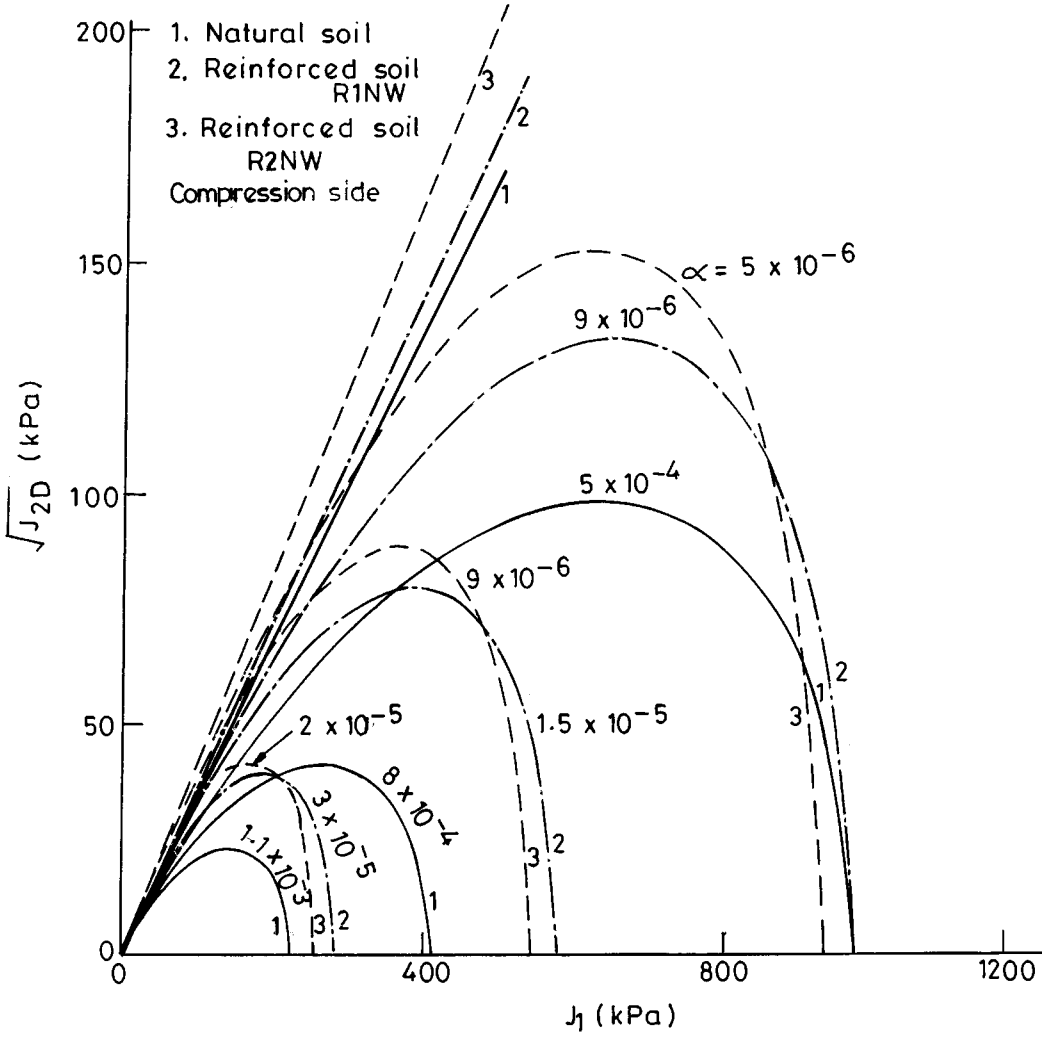

Figure 3. Plot of basic function F_b in the $J_1 - \sqrt{J_{2D}}$ plane for natural soil and reinforced soil, R1NW and R2NW for compression side ($S_r = 1$)

between σ_n and v_r. The material parameters determined from the tests for soil–reinforcement interface is presented in Table III.

For the reinforcement the material parameters given in Table I have been used.

7. PREDICTIONS

The predictions of the natural and reinforced soils have been made by considering natural and reinforced soil as (a) a composite single material and (b) a material consisting of three

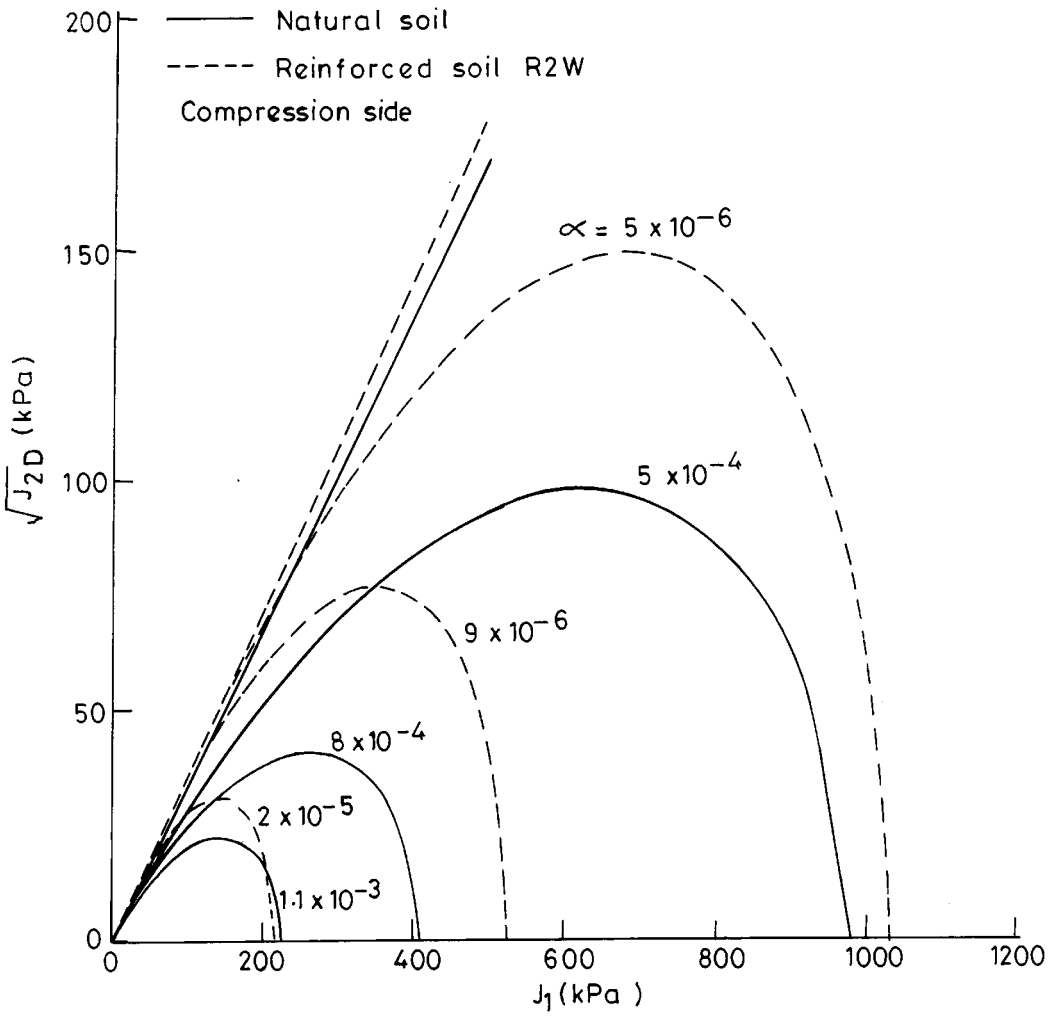

Figure 4. Plot of basic function F_b in the $J_1 - \sqrt{J_{2D}}$ plane for natural soil and reinforced soil, R2W for compression side ($S_r = 1$)

components, viz., soil, reinforcement and interface between soil and reinforcement. The procedures are briefly presented in the following.

The prediction in the first case designated as SPM has been made by integrating the incremental stress–strain relation as

$$\{d\sigma\} = [C^{eP}]\{d\varepsilon\} \tag{19}$$

where $\{d\sigma\}$ and $\{d\varepsilon\}$ are the incremental stress and strain vectors and $[C^{eP}]$ is the elasto-plastic constitutive matrix. Using the theory of plasticity, the incremental plastic strain vector can be

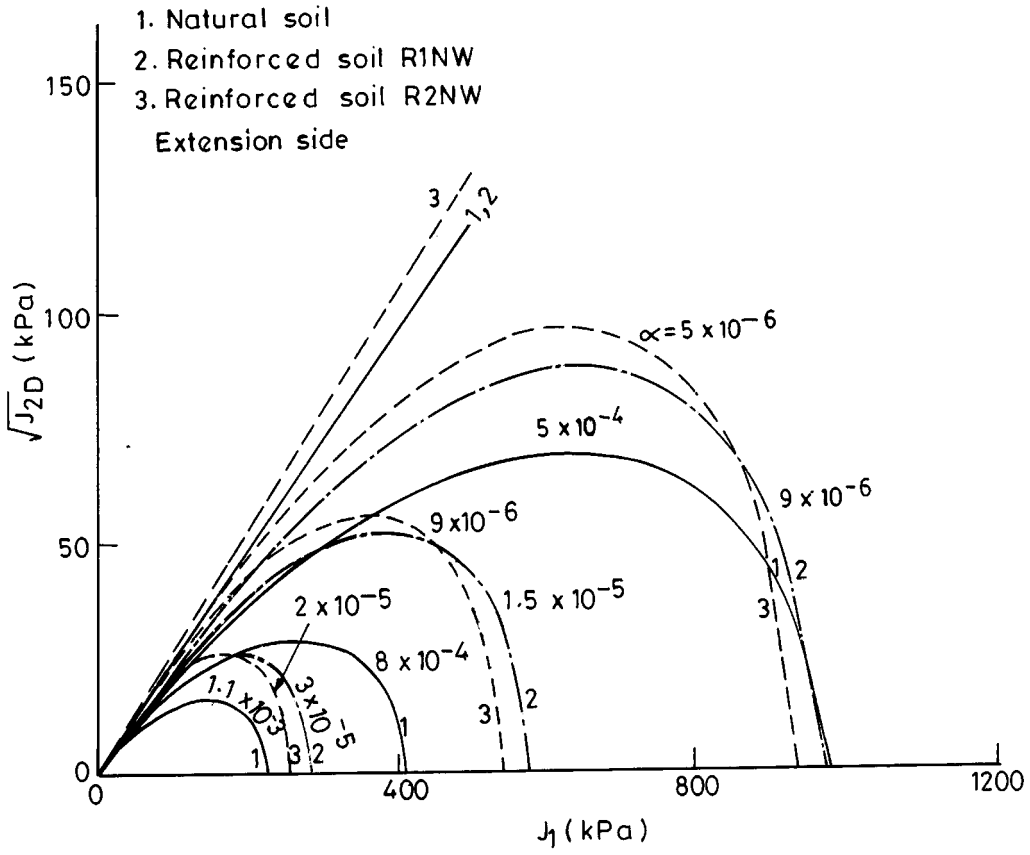

Figure 5. Plot of basic function F_b in the $J_1 - \sqrt{J_{2D}}$ plane for natural soil and reinforced soil, R1NW and R2NW for extension side ($S_r = -1$)

derived from the relation

$$\{d\varepsilon^P\} = \lambda \left\{\frac{\partial Q}{\partial \sigma}\right\} \tag{20}$$

where λ is the scalar constant of proportionality. The incremental stress–strain relationship is derived using the consistency condition $dF = 0$. The material parameters for natural and reinforced soil given in Table II have been used.

The prediction in the second case designated as FEM, the finite element method has been used. The discretization of the reinforced soil, R1NW, under axisymmetric condition with eight-noded isoparametric element for soil and reinforcement and six-noded joint element for soil–reinforcement interface is shown in Figure 2. A similar discretization has been used for R2NW and R2W samples.

To obtain elastoplastic strains, elastoviscoplastic theory has been used.[21] In this approach, it is assumed that all plastic strains (called viscoplastic strains) in the material are developed with

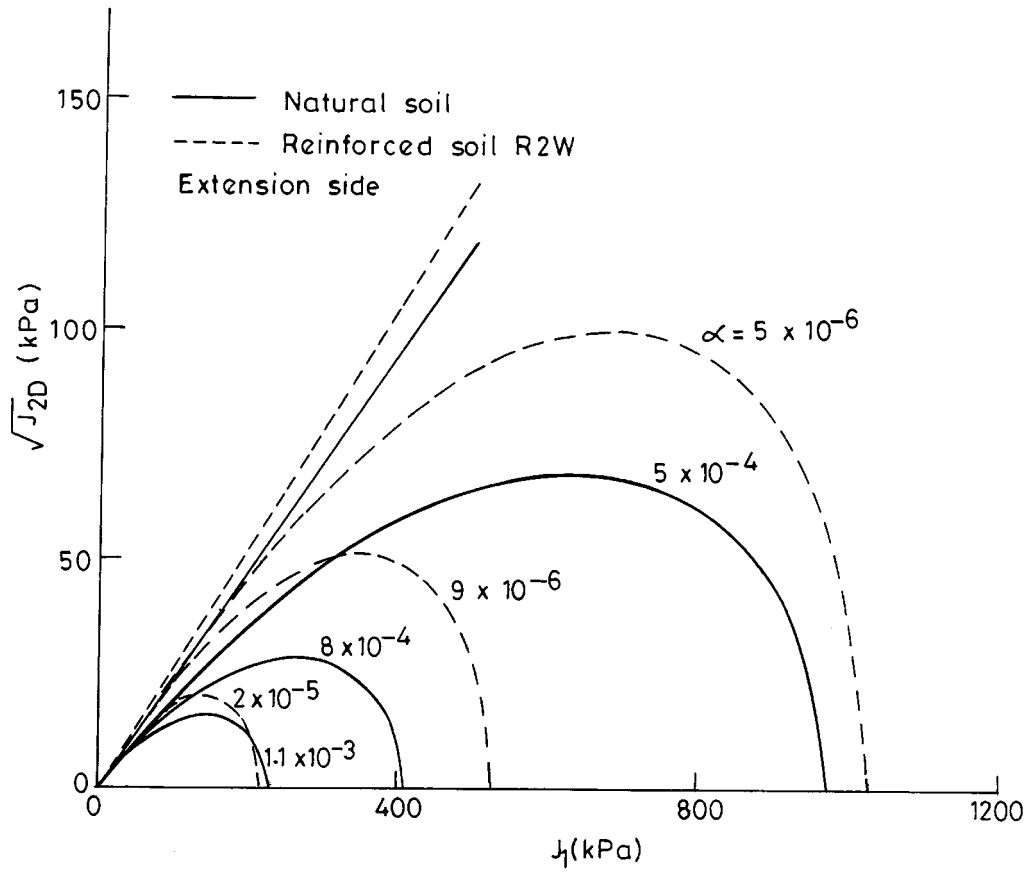

Figure 6. Plot of basic function F_b in the $J_1 - \sqrt{J_{2D}}$ plane for natural soil and reinforced soil, R2W for extension side ($S_r = -1$)

time. The equations of elasto-viscoplasticity are used purely as an artifice to set up a time-marching scheme to get elastoplastic strains. The loading has been applied corresponding to the stress path adopted for testing.

The predictions by SPM have been made for two groups of tests, viz. Group A-tests used for determining material parameters and Group B-tests not used for evaluating material parameters. The finite element method (FEM) has been used for the prediction of all tests.

For Group A and Group B, prediction for one typical test for each group has been chosen for natural soil and reinforced soils R1NW, R2NW and R2W.

8. RESULTS AND DISCUSSIONS

Comparing the value of Young's modulus (E) at $\sigma_3 = p_a$ in equation (16) for k and n' values in Table II, it is observed that (i) with reinforcement, the value of E decreases, (ii) with increase in

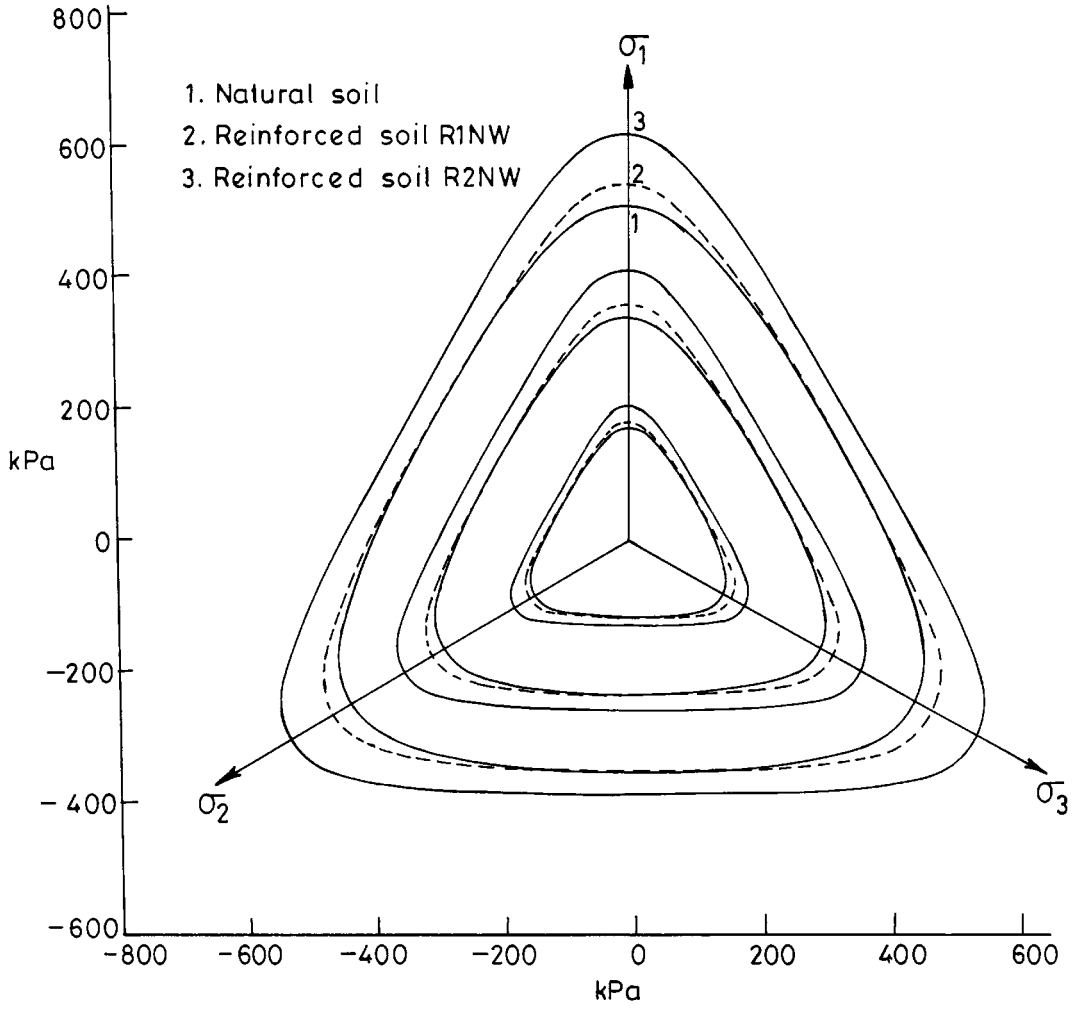

Figure 7. Plot of shape function F_s in the octahedral plane for natural soil and reinforced soil, R1NW and R2NW

number of layers (R1NW and R2NW), the E value decreases and (iii) the non-woven geotextile gives lower E value than the woven geotextile (R2NW and R2W).

In Figures 3–6 are shown the comparison of yield surfaces in $J_1 - \sqrt{J_{2D}}$ stress space for natural and reinforced soils for compression and extension paths. In the figure, the value of growth function α, which is inversely related to plastic strain (equation (4)), signify magnitude of yielding. Lower the value of α, higher is the value of plastic strain denoting increased yielding. Furthermore, lower value of α also leads to higher value of $\sqrt{J_{2D}}$ for the same J_1 value (equation (1)). From the figures, it is found that (i) the reinforcement causes more yielding, (ii) the increase in number of layers results in increased yielding, (iii) compression paths give more yielding with

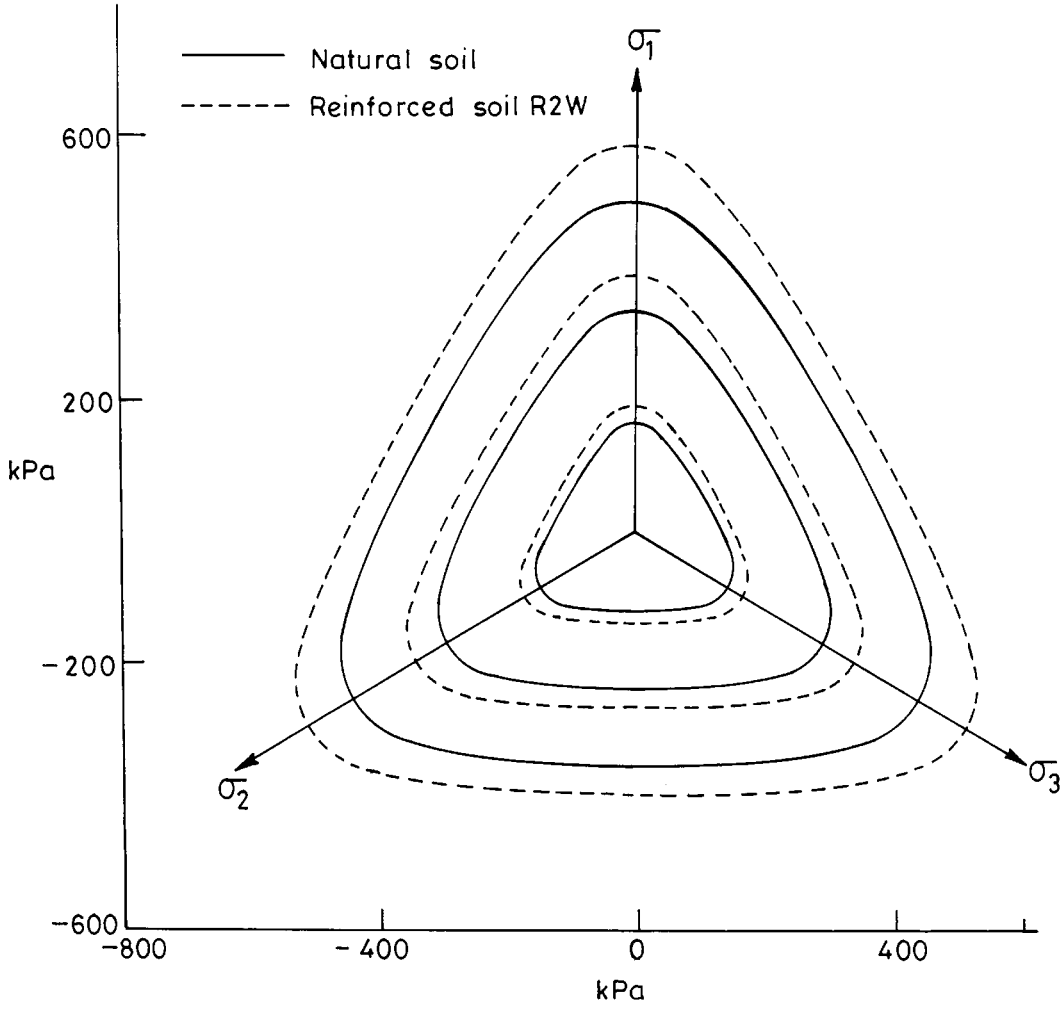

Figure 8. Plot of shape function F_s in the octahedral plane for natural soil and reinforced soil, R2W

respect to natural soil than extension paths, and (iv) the difference in yielding between natural and reinforced soil is higher for higher $\sqrt{J_{2D}}$ values.

Comparing the ultimate lines (at $\alpha = 0$) also shown in Figures 3–6 along with values of γ in Table II, it is observed that (i) as would be expected, the strength increases with reinforcement as well as number of layers of reinforcement, (ii) woven reinforcement gives greater strength than non-woven reinforcement and (iii) the difference is more pronounced for compression path than extension path.

Figures 7 and 8 present comparison of yield surfaces in the octahedral plane at various confining pressures for natural and reinforced soils. The observations made with respect to ultimate lines earlier are also clearly indicated in these figures.

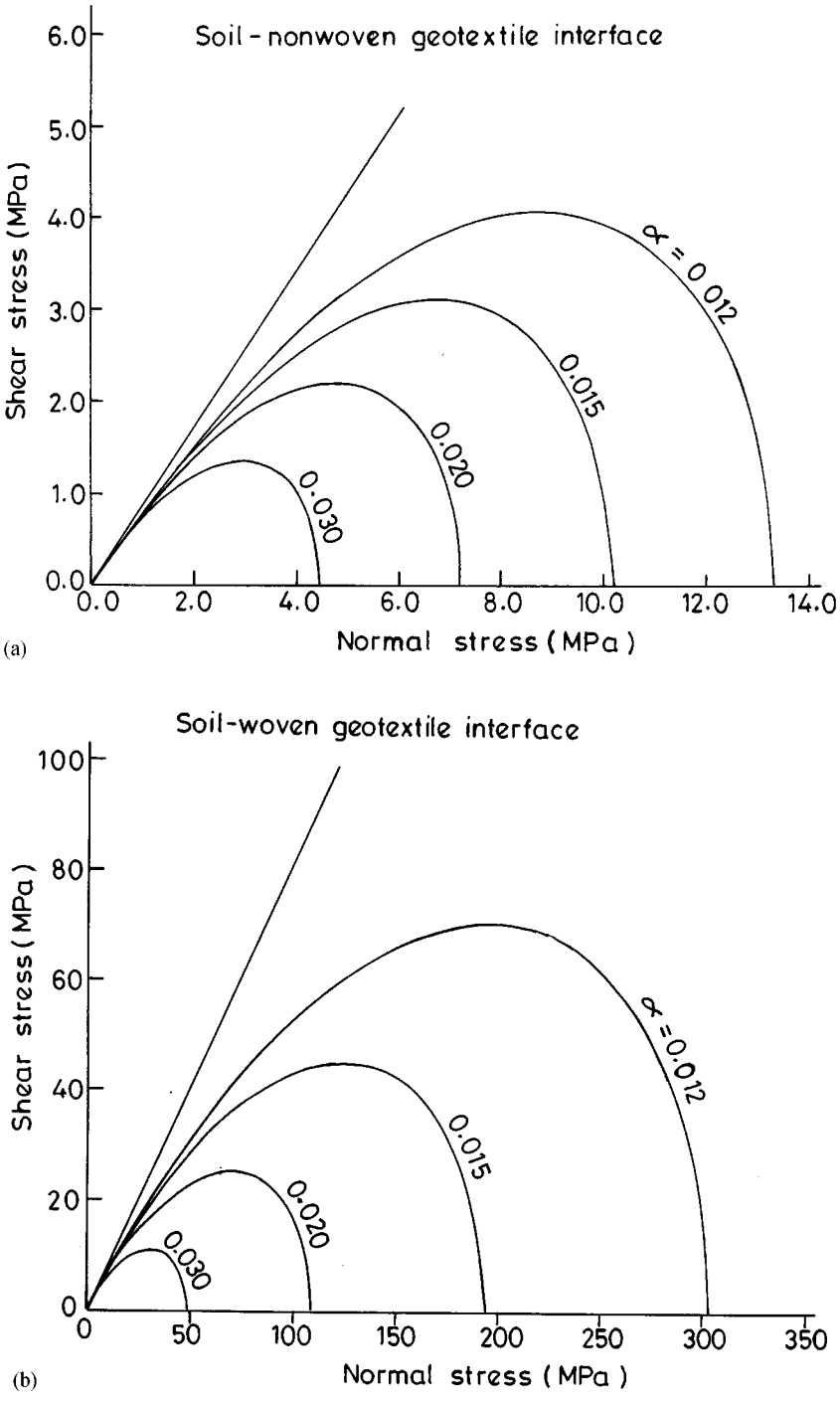

Figure 9. Plot of yield surface for soil–reinforcement interfaces

Table IV. Details of tests used for Group A and Group B predictions

Type of soil sample	Group A tests	Figure nos.	Group B tests	Figure nos.
Natural soil	CTC, $\sigma_c = 200$ kPa	10	RTE, $\sigma_c = 100$ kPa	11
Reinforced soil, R1NW	TE, $\sigma_c = 200$ kPa	12	TC, $\sigma_c = 200$ kPa	13
Reinforced soil, R2NW	TE, $\sigma_c = 200$ kPa	14	RTC, $\sigma_c = 200$ kPa	15
Reinforced soil, R2W	RTE, $\sigma_c = 200$ kPa	16	TC, $\sigma_c = 200$ kPa	17

Note: Predictions by FEM are also made for all the tests and are shown in the same figures.

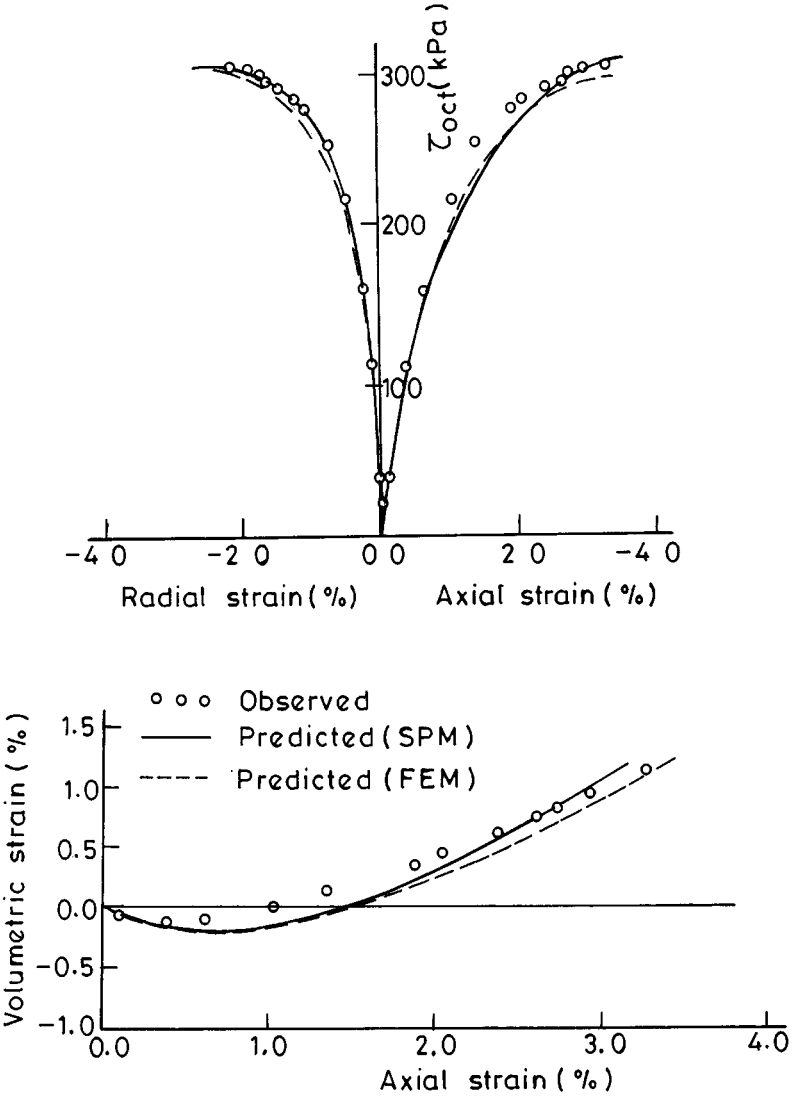

Figure 10. Stress–strain–volume change response of natural soil for CTC path at $\sigma_c = 200$ kPa (Group A)

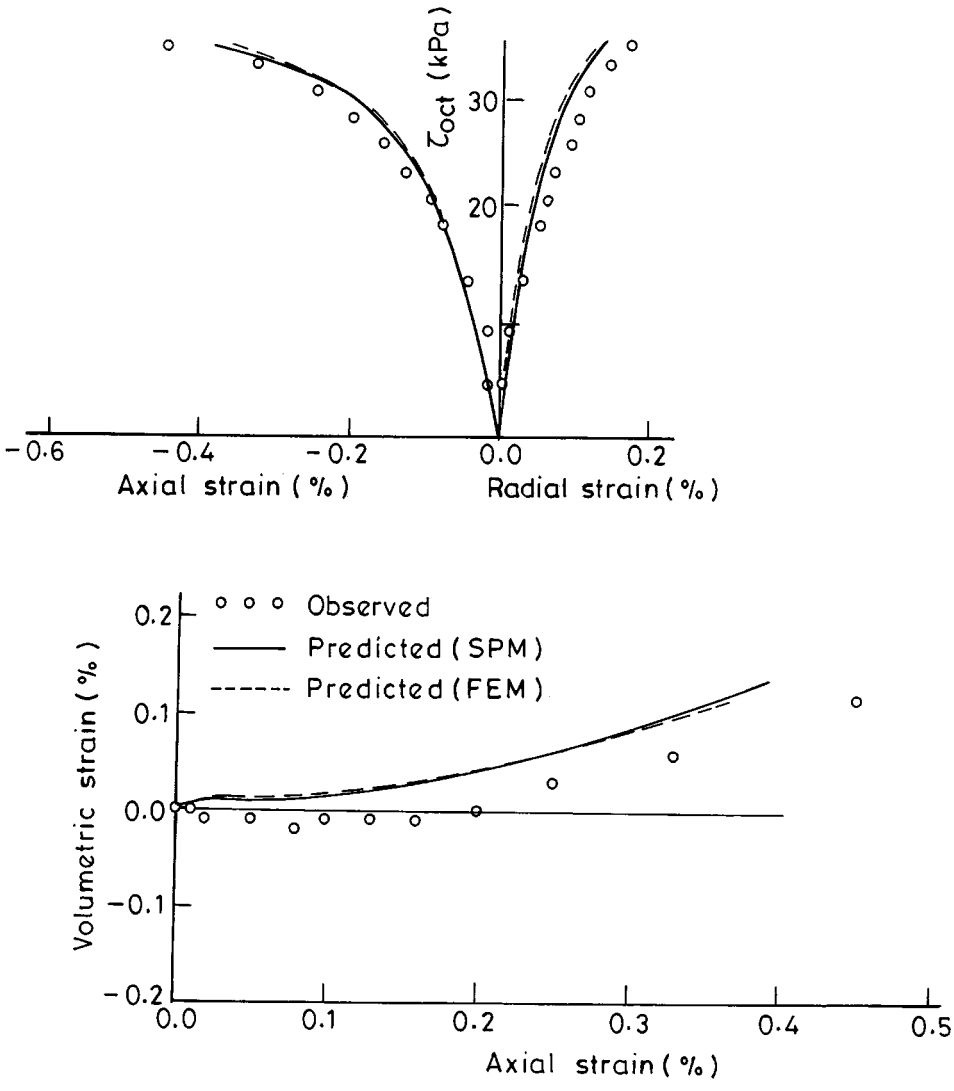

Figure 11. Stress–strain–volume change response of natural soil for RTE path at $\sigma_c = 100$ kPa (Group B)

Comparing the values of phase change parameter, n, (Table II) it is found that n values are higher for reinforced soil samples. Furthermore, non-woven reinforcement shows higher n value than woven reinforcement. Higher n value indicates on set of dilation at higher ratios of J_{2D}/J_1^2 (equation (12)).

Comparison of the hardening parameters a_1 and η_1 shows mobilization of higher plastic strains for reinforced soil samples resulting in lower value of growth function α as shown in Figures 3–6. Non-woven reinforcement gives lower value of growth function, α, than woven reinforcement.

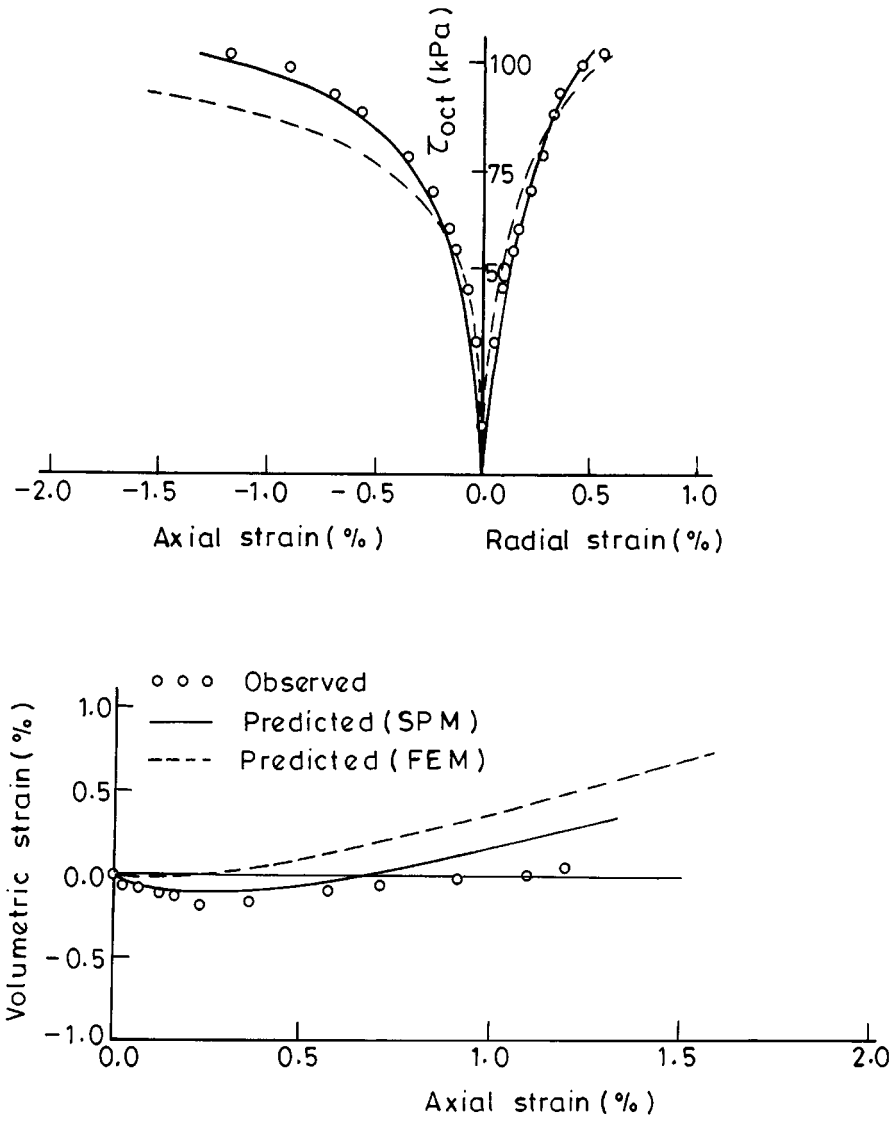

Figure 12. Stress–strain–volume change response of reinforced soil R1NW for TE path at $\sigma_c = 200$ kPa (Group A)

The variation in non-associative parameter κ among natural and reinforced soil samples is very small.

In Figure 9 are shown the yield surface and ultimate line for soil–reinforcement interfaces with non-woven and woven geotextiles. Comparing various parameters at the soil–reinforcement interface (Table III and Figure 9), it is found that non-woven geotextile gives lower elastic modulus values and higher ultimate parameter, phase change parameter and

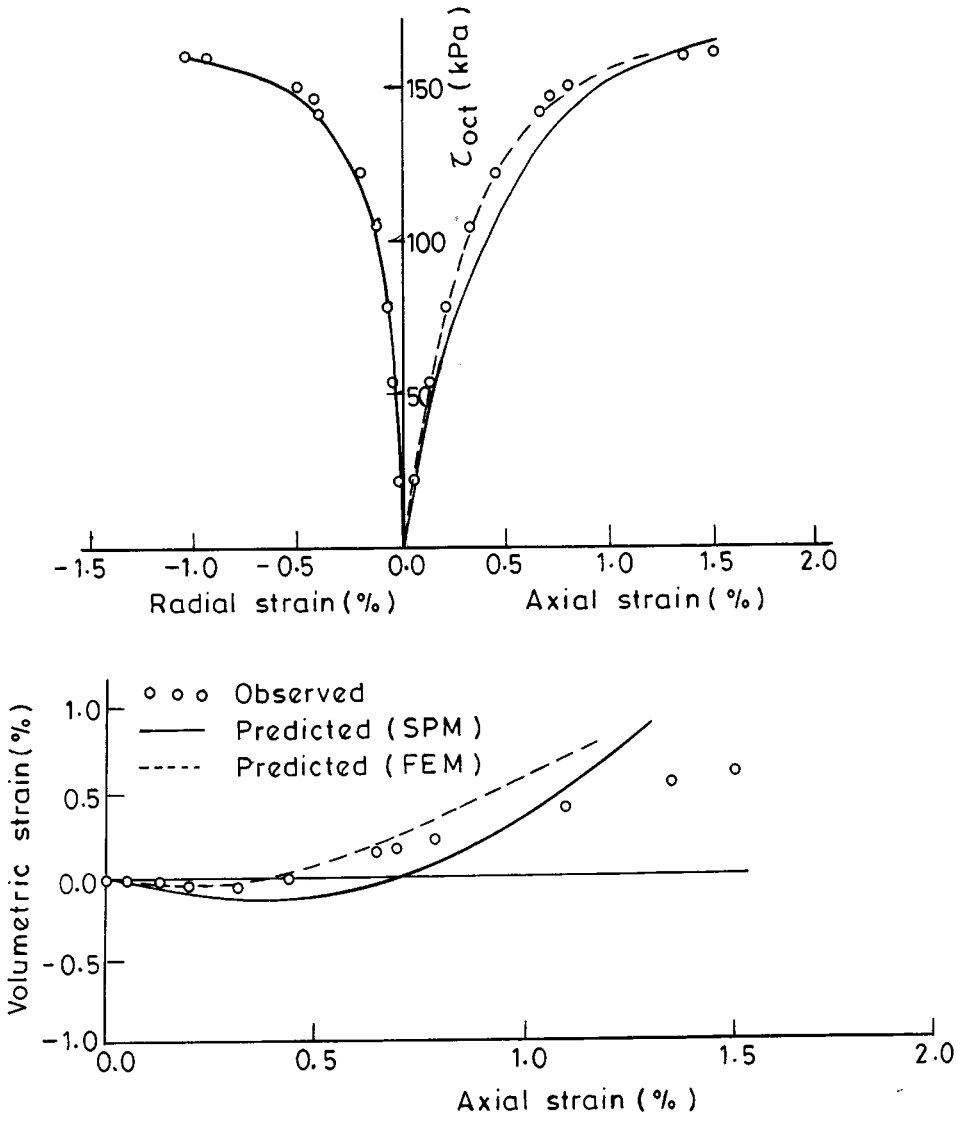

Figure 13. Stress–strain–volume change response of reinforced soil R1NW for TC path at $\sigma_c = 200$ kPa (Group B)

non-associative parameter than woven geotextile. The growth function, α, is lower for non-woven geotextile.

The details of the tests used for Group A and Group B predictions are given in Table IV. The behaviour of these tests have been predicted by FEM as well.

Figures 10 and 11 show comparisons of predictions of stress–strain–volume change behaviour with observed response for natural soil for CTC and RTE paths, respectively. Both SPM and FEM give almost same predictions which are very close to the observed behaviour.

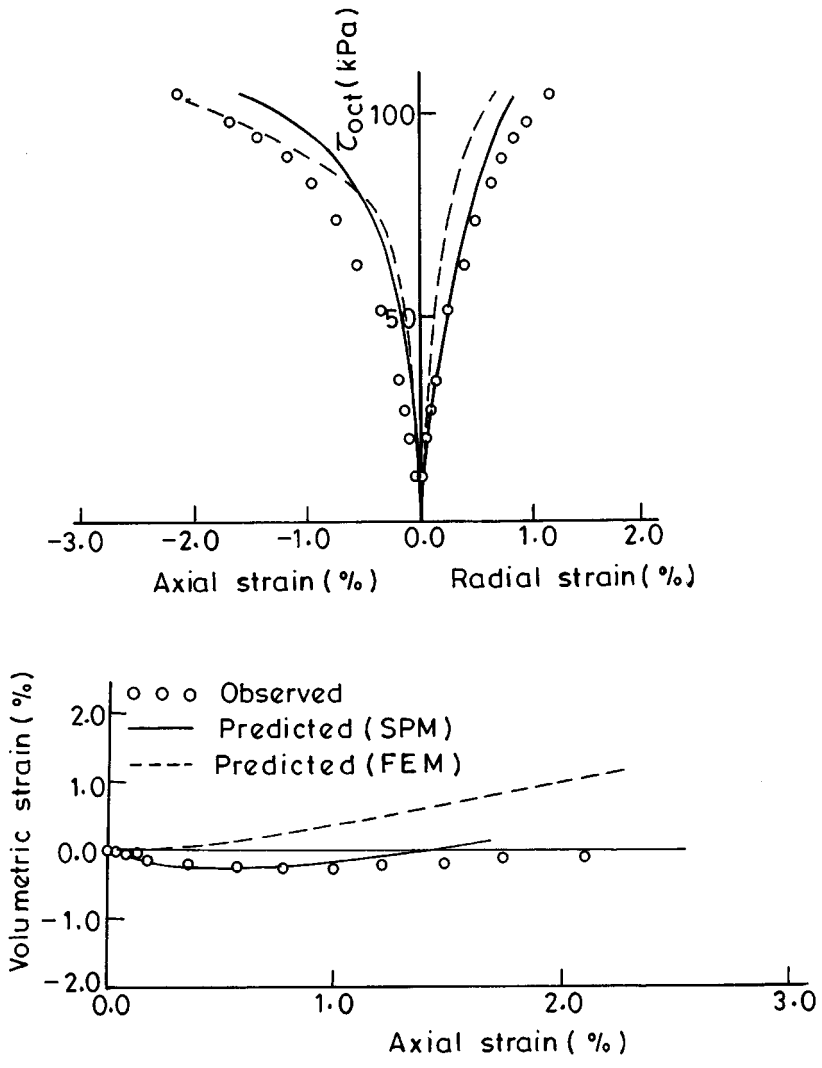

Figure 14. Stress–strain–volume change response of reinforced soil R2NW for TE path at $\sigma_c = 200$ kPa (Group A)

In Figures 12 and 13 are shown comparisons for the reinforced soil for R1NW for TE and TC paths, respectively. Both SPM and FEM provide generally satisfactory predictions. However, SPM shows closer prediction for TE path, and FEM gives better prediction for TC path.

Figures 14 and 15 present comparisons for the reinforced soil R2NW for TE and RTC paths, respectively. The predictions by both approaches are generally satisfactory for this soil also. But, the prediction by SPM is closer to observed behaviour for TE path and FEM shows closer predictions for RTC path.

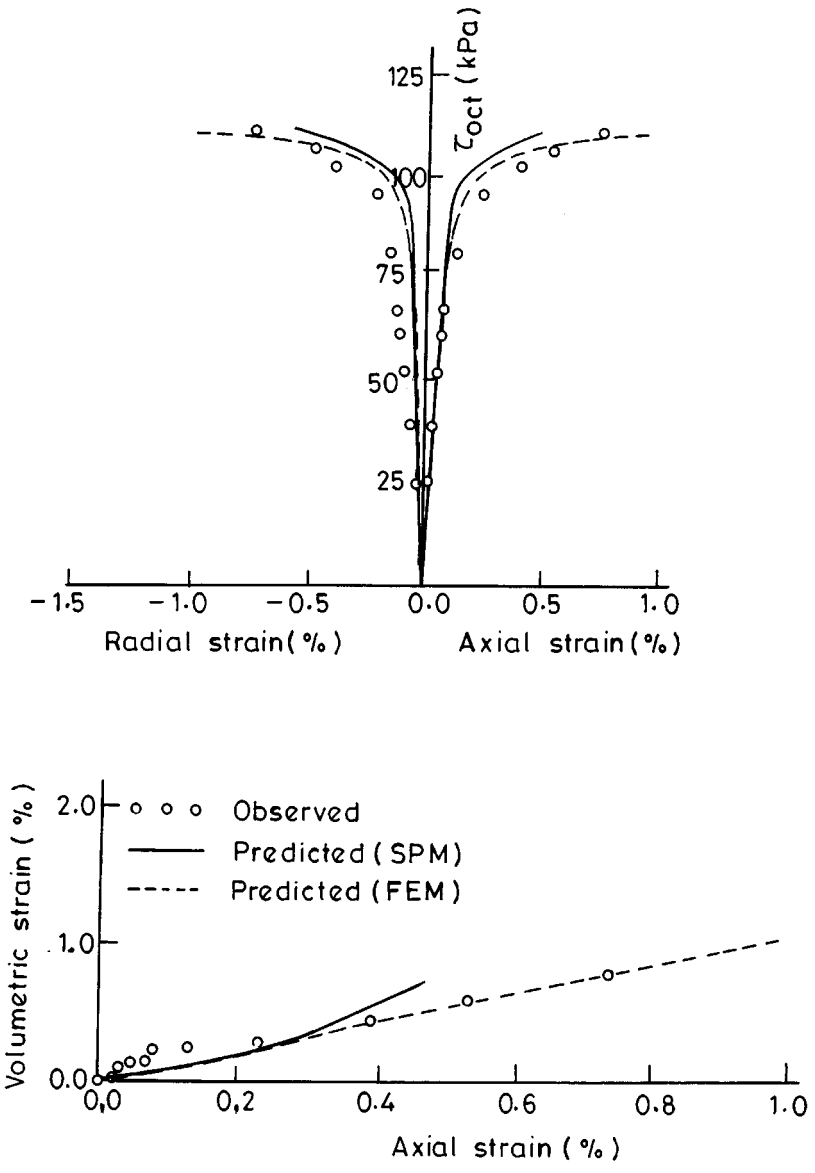

Figure 15. Stress–strain–volume change response of reinforced soil R2NW for RTC path at $\sigma_c = 200$ kPa (Group B)

In Figures 16 and 17 are shown comparison of predictions for the reinforced soil R2W for RTE and TC paths, respectively. For this soil also, both methods provide generally satisfactory predictions. FEM gives relatively closer prediction than SPM for both the stress paths.

From the above comparisons it is found that (i) for natural soil, both the methods provide predictions which are very close to the observed behaviour, (ii) for the reinforced soils, the

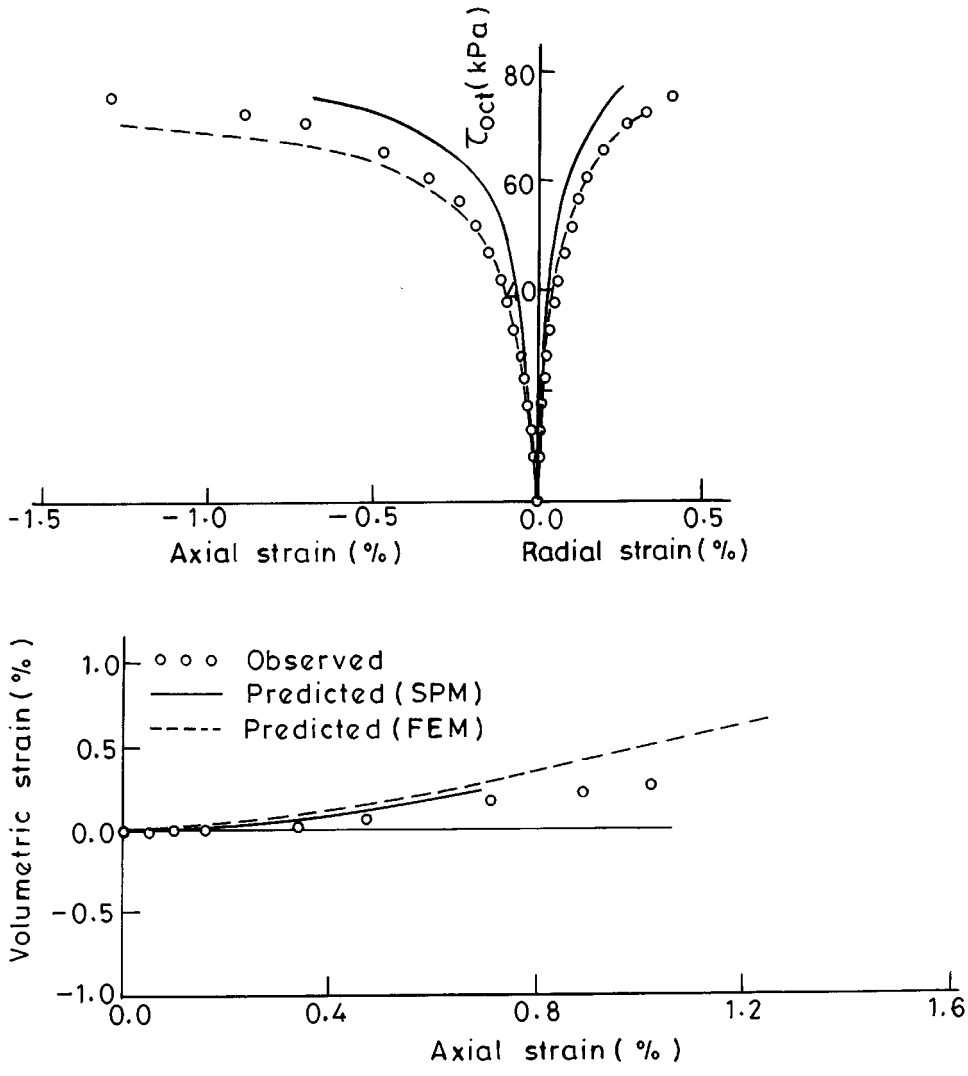

Figure 16. Stress–strain–volume change response of reinforced soil R2W for RTE path at $\sigma_c = 200$ kPa (Group A)

predictions are not as good as for natural soil, but the overall trend is satisfactory and (iii) for reinforced soils, one method provides better prediction than the other for certain tests and no clear trend is established in favour of any one of the two methods.

In the approach used for SPM, the hierarchical single surface model has been adopted with the assumption that the composite reinforced soil behaviour is isotropic. The reinforced soil sample will exhibit anisotropic behaviour when principal stress directions are rotated. Therefore, the model is the present form is not suitable to capture the anisotropic behaviour.

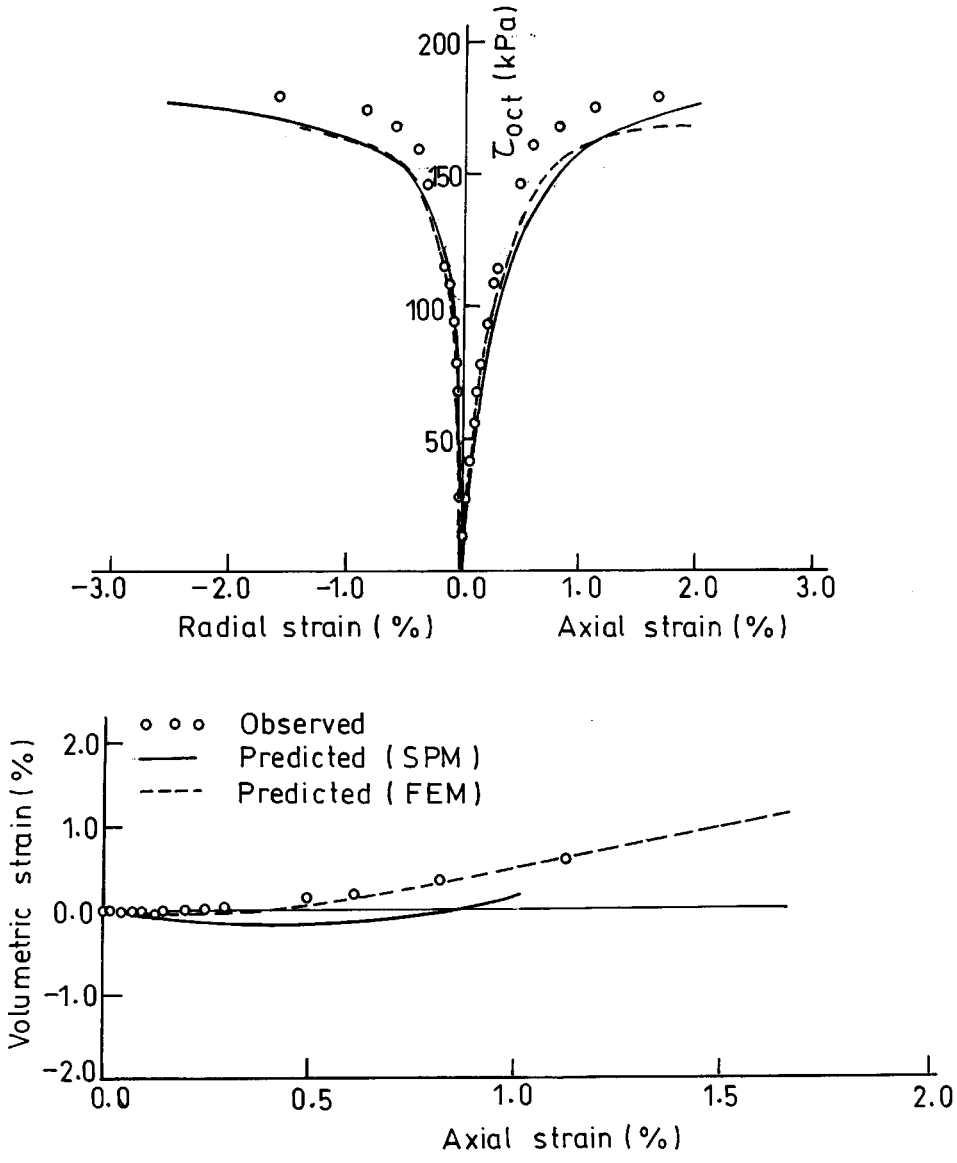

Figure 17. Stress–strain–volume change response of reinforced soil R2W for TC path at $\sigma_c = 200$ kPa (Group B)

The parameters determined in SPM are from the triaxial tests on horizontally reinforced soil samples with the principal stresses in the vertical and horizontal directions. The model with these parameters may be used to analyse those practical problems in which horizontal reinforcement layers are used and the principal stresses remain in the vertical and horizontal directions. Such

a condition prevails in the problems of active and passive cases of reinforced earth retaining structure in an average sense.

In the approach used in FEM since the soil, soil–reinforcement interface and reinforcement are modelled separately, it does not have the limitation of SPM and can capture anisotropic response due to rotation of principal stresses.

9. CONCLUSIONS

Four series of drained triaxial tests have been conducted on natural and reinforced sand samples under six stress paths and various confining pressures. Non-woven and woven geotextiles in the form of circular discs have been used in single and two layers as reinforcement for soil samples. Direct shear tests have been conducted on the interface between soil and reinforcement.

Hierarchical single surface model has been used to characterise the behaviour of natural and reinforced soil samples. Prediction of stress–strain–volume change response has been made by modelling the reinforced soil as a single composite material and by depicting it to consist of soil, reinforcement and soil–reinforcement interface as separate elements in finite element method.

It has been found that the values of ultimate parameters and the phase change parameter increase whereas the value of growth function decreases with reinforcement. The effect of non-woven and woven geotextile reinforcement on soil behaviour is similar in nature. At the soil–reinforcement interface, the effect of non-woven geotextile is more significant than woven geotextile.

The stress–strain–volume change prediction by the hierarchical model is satisfactory by both the approaches used in the study for the triaxial tests on natural and reinforced soils. As such the hierarchical single surface model appears suitable to depict the reinforced soil behaviour.

REFERENCES

1. H. Vidal, 'The principle of reinforced earth', *Highway Research Record*, (282) 1–16 (1969).
2. Z. Yang, 'Strength and deformation characteristics of reinforced sand', *Ph.D. Thesis*, Univ. of California, Los Angeles, USA, 1972.
3. J. Narain, 'Reinforced earth', *Indian Geotech. J.*, **15**(1), 1–25 (1984).
4. K. M. Soni, Constitutive modelling of reinforced soil, *Ph.D. Thesis*, I.I.T. Delhi, India, 1995.
5. A. Sawicki, 'Plastic limit behaviour of reinforced earth', *J. Geotech. Engng. Div. ASCE*, **109**(7), 1000–1005 (1983).
6. M. R. Madhav and H. B. Poorooshasb, 'A new model for geosynthetic reinforced soil', *Comput. Geotech.*, **6,** 277–290 (1988).
7. P. de Buhan and L. Siad, 'Influence of soil strip interface failure condition on the yield strength of reinforced earth', *Comput. Geotech.*, **7,** 3–18 (1989).
8. P. L. Bourdeau, 'Modelling membrane action in a two layer reinforced soil system', *Comput. Geotech.*, **7,** 19–36 (1989).
9. A. W. Bishop and D. J. Henkel, *The Measurement of Soil Properties in the Triaxial Test*, Edward Arnold Ltd., London, 1957.
10. G. V. Rao and S. K. Pandey, 'Evaluation of geotextile soil friction', *Indian Geotech. J.*, **18**(1), 77–105 (1988).
11. C. S. Desai 'A general basis for yield, failure and potential function in plasticity', *Int. J. Numer. Anal. Meth. Geomech.*, **4,** 361–375 (1980).
12. C. S. Desai, S. Somasundaram and G. Frantziskonis, 'A hierarchical approach for constitutive modelling of geologic materials', *Int. J. Numer Anal. Meth. Geomech.*, **10**(3) (1986).
13. C. S. Desai, 'Hierarchical single surface and disturbed state constitutive models with emphasis on geotechnical applications', in K. R. Saxena (ed.), *Geotechnical Engineering*, Oxford & IBH Publ. Co., Delhi, 1994.
14. G. Frantziskonis, C. S. Desai and S. Somasundaram, 'Constitutive model for non-associative behaviour', *J. Engng Mech. Div. ASCE*, **112**(9), 932–946 (1986).
15. C. S. Desai and K. L. Fishman, 'Plasticity based constitutive model with associative testing for joints', *Int. J. Rock Mech. Min. Sci. & Geomech. Abstr.*, **28**(7), 15–26 (1991).

16. C. S. Desai and G. W. Wathugala, 'Hierarchical and unified models for solids and discontinuities (Joints/interfaces), in C. S. Desai (ed.), *Implementation of Constitutive Laws for Engineering Materials*, *Short Course Notes*, Univ. of Arizona, Tucson, USA, 1987.
17. K. G. Sharma and C. S. Desai, 'Analysis and implementation of thin layer element of interfaces and joints', *J. Engng Mech. Div. ASCE*, **118**(12)**,** 2442–2462 (1992).
18. A. Varadarajan and C. S. Desai, 'Material constants of a constitutive model, Determination and use', *Indian Geotech J.* **23**(3)**,** 291–313 (1993).
19. N. Janbu, 'Soil compressibility as determined by Oedometer and triaxial texts', *Eur. Conf. on SMFE*, Weisbaden, Germany, Vol. 1, 1963, pp. 19–25.
20. K. L. Fishman, 'Constitutive modelling of idealised rock joints under quasi-static and cyclic loading', *Ph.D. Thesis*, University of Arizona, Tucson, USA, 1988.
21. I. C. Cormeau, 'Numerical stability in quasistatic elasto-viscoplasticity', *Int. J. Numer meth. Engng*., **9,** 109–128 (1975).

